Local cation environments in the pyrope–grossular $Mg_3Al_2Si_3O_{12}$–$Ca_3Al_2Si_3O_{12}$ garnet solid solution

Colin L. Freeman and Neil L. Allan
School of Chemistry, University of Bristol, Cantock's Close, Bristol BS8 1TS, United Kingdom

Wim van Westrenen
Faculty of Earth and Life Sciences, Vrije Universiteit, De Boelelaan 1085, 1081 HV Amsterdam, The Netherlands
(Received 28 December 2005; published 5 October 2006)

We report *ab initio* calculations of the highly nonideal pyrope ($Mg_3Al_2Si_3O_{12}$)–grossular ($Ca_3Al_2Si_3O_{12}$) garnet solid solution. The results highlight the crucial influence of the *local* environment of individual cations on the structure and energetics of the solution. The energies of particular atomic configurations are closely related to the third nearest neighbor arrangement of the Mg and Ca cations, even though third nearest neighbors are typically separated by as much as ≈6 Å. The non-ideality, the local cation environment and the distortions of the SiO_4 tetrahedra which separate third nearest neighbors are all linked. The small size of the Mg ion, particularly when part of a third neighbor Mg-Mg pair, is the principal factor responsible for distortion in the garnet framework. The third neighbor interactions also have a dramatic influence on the energetics of the incorporation of foreign ions in the solid solution. Our calculations indicate that the length of the cation-O1 bond is largely independent of solid solution composition. In contrast, that of the longer cation-O2 bond varies almost linearly with composition, increasing with increasing Ca content. The lengths of the Mg-O2 and Ca-O1 bonds become more similar as the Mg mole fraction rises but at the 50:50 composition there is still an appreciable difference (≈0.1 Å), and a difference is still present even close to the dilute limit, in apparent disagreement with recent extended x-ray-absorption fine structure (EXAFS) experiments.

DOI: 10.1103/PhysRevB.74.134203 PACS number(s): 61.50.Ah, 92.20.Wx, 72.80.Ng

I. INTRODUCTION

Solid solutions, particularly of oxides, and grossly disordered minerals continue to present considerable challenges to the theoretician. In particular, details of how crystal structure and dynamics and *local* structural distortions give rise to non-ideality remain largely uncertain. In this paper, we concentrate on the non-ideality of garnet ($X_3Y_2Z_3O_{12}$, where X, Y, and Z are cations), which is an abundant rock-forming mineral in the Earth's crust, upper mantle, and transition zone. Garnet solid solutions are stable over a wide range of temperatures (T) and pressures (P). Coupled with systematic variations in solid solution composition as a function of P and T, this makes them very useful for modeling rock formation and evolution conditions. Building up a detailed understanding of the garnet solid solution is vital if these efforts are to be successful, as well as of fundamental interest to those developing general models of solid solutions of ionic and semi-ionic oxides and silicates.

We focus on two particular garnet end members, pyrope ($Mg_3Al_2Si_3O_{12}$) and grossular ($Ca_3Al_2Si_3O_{12}$) and the solid solution they form together. Previous studies have shown the pyrope-grossular solid solution to be highly non-ideal (e.g., Refs. 1–4 and references therein). The detailed atomistic behavior responsible for this non-ideality is still not understood. So-called hybrid models which are essentially mean-field treatments are very unsuccessful (e.g., Ref. 10). The non-ideality is clearly dependent on the complex crystal structure (Fig. 1). This is best viewed as a set of connected polyhedra: SiO_4 form tetrahedra that corner share with the AlO_6 octahedra; the Mg and Ca cations form distorted dodecahedra with the eight nearest O and these share edges with the SiO_4 tetrahedra and AlO_6 octahedra. The cation-oxygen bonds are divided into two groups of four, cation-O1 and the significantly longer cation-O2 (by ≈0.15 Å for both pyrope and grossular). The O1 atoms are all shared with the Si, while the Al share one O1 and one O2. The Mg^{2+} cation

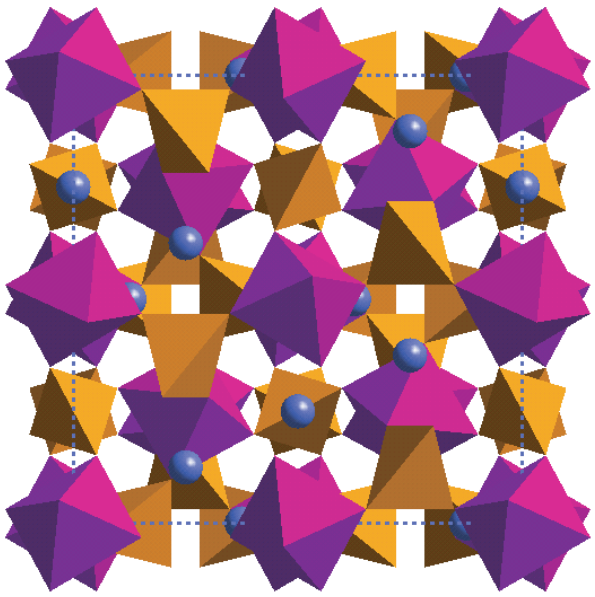

FIG. 1. (Color online) The garnet unit cell. Here and in the remainder of the figures, SiO_4 tetrahedra are depicted in yellow (light gray), Al octahedra in purple (dark gray), and cations (Ca and Mg) in blue (dark gray circles). For simplicity, oxygen atoms are not shown.

is rarely found in eightfold coordination due to its small size, which makes the local environment of the Mg cation in garnet particularly interesting and unusual. The interconnected, relatively dense lattice means that the nature of the dodecahedral cations significantly influences the positions of the surrounding atoms, i.e., the local structural environment.

Early refinements of the crystal structure showed that all the polyhedra are distorted from their ideal shape.[5] Vibrational spectroscopy has observed distortions in the SiO_4 tetrahedra in the solid solution as the mole fraction of Mg increases.[1] Ungaretti *et al.*[6] have reported *average* O-Si-O bond angles of 109.61° and 109.54° in pyrope and grossular respectively; both values are a little above the ideal or regular tetrahedral angle of 109.47°. A larger difference is observed between the end members for the Al-O than the Si-O bond lengths[6] since the Al-O bond is less rigid and this leads to a distortion in the AlO_6 octahedra. Potential-based calculations[7] on the end members also suggest the edges of the SiO_4 tetrahedra are distorted. Calculated lengths of the tetrahedral edges shared with the Mg and Ca cation dodecahedra are smaller than the other unshared edges thus compressing the associated O-Si-O angles from the ideal tetrahedral value, even though the average O-Si-O angle increases.

There is some debate over the variation of the cation-O bond lengths in the pyrope-grossular solid solution with Mg content. The x-ray absorption fine structure (XAFS) and x-ray absorption near-edge structure (XANES) data of Quartieri *et al.*[8] suggest that the local geometry of the divalent dodecahedral cation at the *X*-site is dependent on the overall composition of the solid solution. More recent extended x-ray-absorption fine structure (EXAFS) studies of Oberti *et al.*[9] report a nonlinear decrease in Ca-O1 and Ca-O2 bond lengths with increasing Mg content in the solid solution, resulting in a convergence of the Ca-O1 and Ca-O2 bond lengths with the Mg-O2 bond for mole fractions <0.5 grossular. In contrast, classical simulations[7,10] have suggested that "cations *largely* preserve their local environment in the solid solution, even in the dilute limit." These calculations conclude that a Ca cation in a predominantly pyrope solid solution maintains grossularlike Ca-O bond lengths and similarly a Mg cation in a predominantly grossular solid solution adopts Mg-O bond lengths close to those in pyrope.

The results of ^{29}Si NMR studies by Bosenick *et al.*[11,12] suggest that the *X*-site cations in the pyrope–grossular solid solution are not randomly distributed. Their studies demonstrate a short range cation ordering which decreases with increasing temperature. Monte Carlo[7] and also static energy simulations[10] have been used to examine the *X*-site cation ordering; see also Vinograd *et al.*[13] The nearest neighbor (NN) cation arrangement is shown in Fig. 2. Each cation has four first-NN, eight second-NN, and two third-NN cations. The third-NN interaction involves two cations separated by a SiO_4 tetrahedron and the corresponding distance is comparatively large ($\approx$5.8 Å). Nevertheless simulations have demonstrated[7,10] a preference for a given cation to avoid an identical cation as its third-NN, resulting in low temperature ordering. When a Ca(Mg) cation has two Ca(Mg) cations as its third-NNs, the energy of the configuration is higher than when a Ca(Mg) has two Mg(Ca) cations as its third-NNs. Surprisingly, despite the smaller separations and larger number of neighbors, the classical simulations suggest the first- and second-NN cation arrangements have considerably less influence on the energy of a configuration than the third-NNs.[7,10]

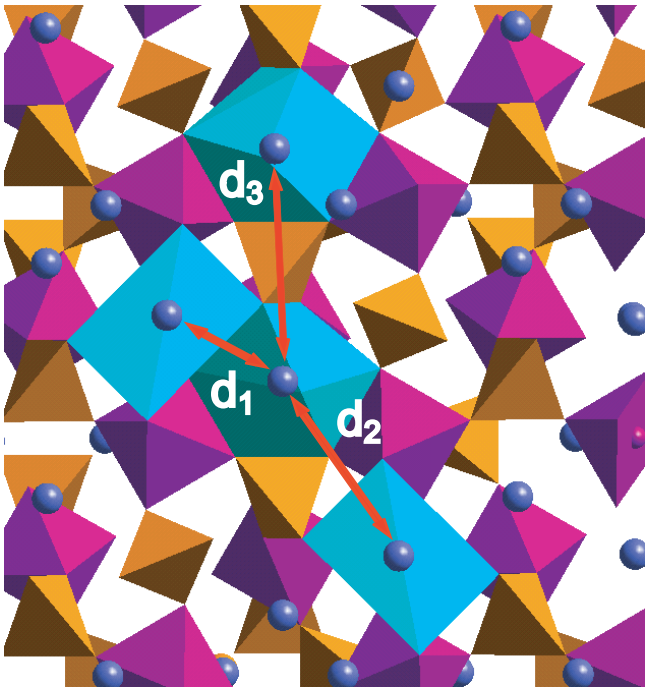

FIG. 2. (Color online) Arrangement of the *X*-site cation-cation first, second, and third-nearest neighbors. Cations (blue atoms) are shown within their dodecahedra (light blue). The first, second, and third-nearest neighbor (NN) distances between the cations are marked as d_1 ($\approx$3.6 Å), d_2 ($\approx$5.4 Å) and d_3 ($\approx$5.8 Å) respectively.

The non-ideality of the garnet solid solution, the local environment of the cations and SiO_4 tetrahedra, and the third-NN cation interactions thus all appear to be linked. Theoretical studies of solid solutions offer the advantage of examining atomic level behavior directly, which can be invaluable in understanding the root causes of the macroscopic behavior. The third-NN interaction has previously so far only been demonstrated with classical potential-based methods. We investigate the local structure in garnet solid solutions through first-principles quantum mechanical (QM) calculations. QM-based methods have proved successful[14–17] in modeling the bulk physical properties of garnet end members, with results in good agreement with experiment. Modeling the garnet solid solution explicitly allowing for different third-NN interactions requires the use of a cubic unit cell with a minimum of 160 atoms, twice the size of the end member primitive rhombohedral unit cell and thus first-principles calculations are particularly computationally expensive. The only two previous QM studies of garnet solid solutions we have been able to find are the recent work of Sluiter *et al.*,[4] also on the pyrope-grossular system, who report impressive results for calculated enthalpies of mixing and miscibility gaps, but do not discuss the local structure (the primary concern of the present paper), and a very brief reference in passing in Ref. 7 to calculations used only to check the parameters in a model Hamiltonian.[18]

II. METHODS

In the primitive rhombohedral end member unit cell only the first- and second-NN cations are present and each cation is effectively third-NN to its periodic image in an adjacent cell. Thus we used the cubic 160 atom cell containing 24 Mg/Ca cations, as shown in Fig. 1. Each cation has one of its third-NNs present within the same unit cell and the other is generated by the periodicity. This means the two third-NNs of each cation must be identical. Thus the cations can be arranged with two third-NNs of the same cation species, i.e., Mg with two Mg cations as third-NNs (Mg-Mg) or Ca with two Ca third-NNs (Ca-Ca). Alternatively the cations can be arranged with two third-NNs of the other cation species, i.e., Mg with two Ca cations as third-NNs (Mg-Ca) or Ca with two Mg cations as third-NNs (Ca-Mg), which are effectively identical. Since each third-NN interaction involves two cations present in the unit cell, in total there are 12 unique third-NN interactions involving cations in the 160-atom unit cell. For example, for a 50:50 Ca:Mg composition, there are 12 Ca and 12 Mg cations; if we have two Ca-Mg third-NNs, this will involve four cations (two Mg and two Ca) and the remaining 20 cations will be arranged with identical third-NNs making five Mg-Mg and five Ca-Ca third-NNs.

Optimizations were carried out with both QM and classical methods on the end members, pyrope and grossular, as well as thirteen 50:50 pyrope–grossular configurations. Configurations were selected to provide a mix of different third-NN arrangements, from the minimum of zero Ca-Mg combinations (where there are six Ca-Ca and six Mg-Mg) to the maximum 12 Ca-Mg. Optimizations were also performed on two configurations for the 25:75, 75:25 pyrope–grossular mixes and one configuration for the 4:96 and 96:4 mixes (as there is only one unique configuration) in order to examine variations in the local cation environment as a function of solid solution composition in more detail. All classical simulations were static energy structural optimizations of the type described in full detail in Ref. 10.

The *ab initio* calculations were performed with the density functional theory (DFT) code CASTEP.[19] Our calculations used the generalized gradient approach (GGA) with the Perdew-Wang exchange-correlation functional.[20] Ultrasoft Vanderbilt pseudopotentials[21] with an energy cutoff of 380 eV were applied. The Monkhorst-Pack sampling scheme[22] was used for the reciprocal space integration; satisfactory convergence was achieved with one k point.

III. RESULTS AND DISCUSSION

A. Pyrope and grossular end members

Calculated bond lengths, unit cell parameters, and bulk moduli from the *ab initio* calculations carried out in this work are compared with experimental values[23,24] in Table I. There is good agreement with experiment. Calculated lattice parameters are ≈0.2% smaller than observed, while bulk moduli are overestimated by ≈8% and ≈2% for pyrope and grossular respectively.

For our present purposes, we need to examine the structure of the end members in more detail. Figure 2 shows that the edge-sharing SiO_4 tetrahedra and XO_8 dodecahedra effectively form one-dimensional (1D) chains running along each unit cell vector (a, b, and c). The X-site cations separated by the SiO_4 tetrahedra are third-NN to each other. Figure 3 shows the structure around the SiO_4 tetrahedra and labels the set of interatomic distances A–D, calculated average values of which are recorded in Table II. The lattice parameter of the grossular unit cell is 3.4% larger than the lattice parameter of the pyrope unit cell and there is a ≈3.3% difference between the Si-X separation (D) in grossular and pyrope. Due to the strength of the Si-O bonds, the SiO_4 tetrahedra are relatively rigid and hard to stretch or compress so the Si-O bond length varies only slightly (by ≈0.015 Å) from grossular to pyrope. Thus, as previously suggested in the QM study of pyrope and grossular of Nobes *et al.*,[16] the structure adjusts to accommodate the differently sized Ca and Mg cations mainly by changes of framework bond angles rather than bond lengths.

In both end members the tetrahedral edges shared with the dodecahedra (distance A) are shorter than the unshared edges, in agreement with the experimental measurements of Ungaretti *et al.*[6] As a result, the two shared oxygens move

TABLE I. Comparison of selected calculated (this work) and experimental X-site cation and other bond lengths and bulk properties for the pyrope[23] and grossular[24] end members.

	Pyrope		Grossular	
Property	Experiment	Calculation	Experiment	Calculation
X-O1 (Å)	2.197	2.203	2.322	2.319
X-O2 (Å)	2.348	2.363	2.487	2.513
Si-O (Å)	1.627	1.616	1.646	1.628
Al-O (Å)	1.889	1.873	1.926	1.918
a (Å)	11.455	11.432	11.848	11.825
K_T (GPa)	171	185	168	171

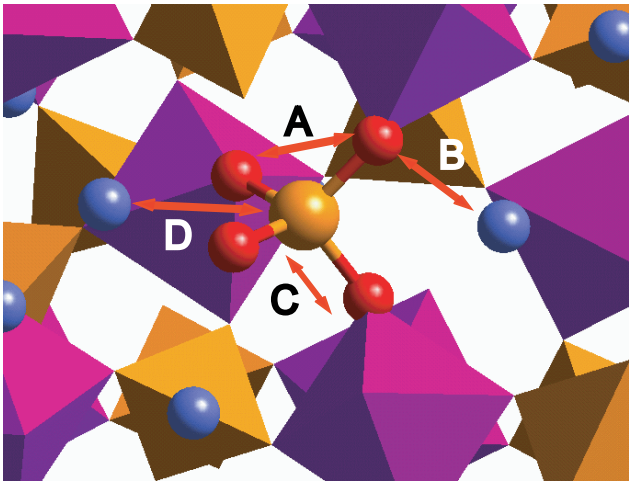

FIG. 3. (Color online) The arrangement of the SiO_4 tetrahedra and the two third-NN cations. The calculated average values of the labeled interatomic distances shown are recorded for pyrope and grossular in Table II.

TABLE II. Calculated average interatomic separations (Å) in the SiO_4 tetrahedra in the end members, grossular and pyrope. The distances *A*–*D* are labeled in Fig. 3.

	Pyrope	Grossular
A (O-O)	2.479	2.543
B (*X*-O1)	2.203	2.319
C (Si-O)	1.616	1.628
D (Si-*X*)	2.858	2.956

closer to each other and to the *X*-site cation (distances *A* and *B*). Calculated values of the resulting bond angles of the SiO_4 tetrahedra, as defined in Fig. 4, are recorded in Table III. The contraction of the tetrahedral edges reduces the O-Si-O angles adjacent to the cations (θ and ϕ) from the ideal tetrahedral value of 109.47°, and increases the four other O-Si-O angles (all labeled φ). We note that the calculated mean O-Si-O angles in pyrope and grossular are 109.60° and 109.54° respectively, in excellent agreement with the experimental values[6] of 109.61° and 109.54°.

Our calculations find the smaller Mg cation forms Mg-O bonds that are ≈5.1% shorter than the Ca-O bonds in grossular. To accommodate the shorter bonds, the distortions of the framework described above are larger in pyrope than in grossular. The O-O separation is ≈2.5% less and θ and ϕ are ≈2.5° smaller in pyrope than in grossular. We summarize the distortions of the tetrahedra using the mean magnitudes of the deviation of the O-Si-O angles from 109.47°, given in the final row of Table III. The mean deviation for pyrope is ≈2° larger than the mean deviation for grossular. The larger framework distortion observed for pyrope agrees with earlier *ab initio* calculations[16] and experiment.[6] It is also worth noting that an examination of the potential energy surface finds only *one* minimum energy position for a Mg cation within a pyrope dodecahedron. This is fully consistent with the *ab initio* results of Nobes *et al.*[16] and does not support earlier suggestions, relating to the so-called excess entropy of pyrope,[25] of a number of "off-center" symmetrically equivalent minima for each Mg.[26]

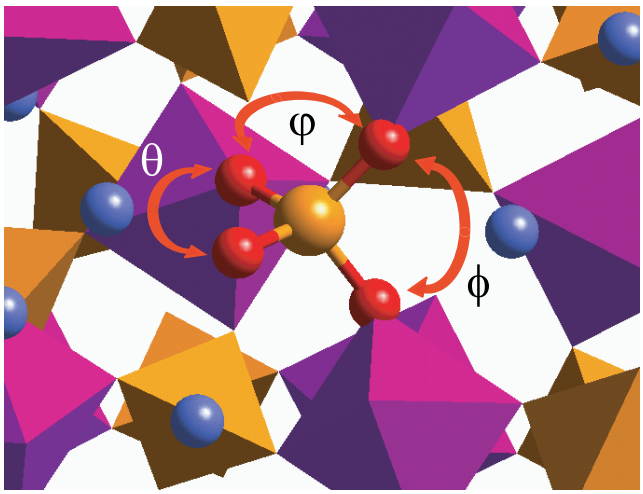

FIG. 4. (Color online) Definition of the bond angles θ, ϕ, and φ. Calculated values are listed in Table III.

TABLE III. Calculated average values of the O-Si-O bond angles (in degrees) shown in Fig. 4.

	Pyrope	Grossular
θ	100.14	102.71
ϕ	100.13	102.71
φ	114.33	112.96
Mean deviation from 109.47° (see text)	6.35	4.58

B. Solid solution: Structure

Before considering the energetics of different configurations, we discuss first the local structural environment of the *X*-site cations in the solid solution. Figure 5 shows the variation of the mean bond lengths *X*-O1 and *X*-O2 in the solid solution for the compositions studied. Note that the results for the 25% and 75% compositions are based on only two configurations but these values are also included to guide the eye. The shorter *X*-O1 bonds (for *both* *X*=Mg and Ca) are rigid and maintain a virtually constant value for all compositions even in the dilute limit. There is a much larger variation for *X*-O2, again for both, *X*=Mg and Ca. The longer *X*-O2 bond length varies almost linearly with solid solution composition, from 2.36 Å in pyrope to 2.50 Å (Mg:Ca 4:96) for Mg-O1 and from 2.51 Å in grossular to 2.41 Å (Mg:Ca 96:4) for Ca-O2. We have checked that the trends in these values agree well with those obtained[27] from classical simulations with the same interionic potentials as used previously.[10]

We are now in a position to comment on the disagreement in the literature of the effect of the bulk composition of the solid solution on the local environment of the *X*-site cation, and specifically the variation in the *X*-O bond lengths. Considering *only* the four nearest oxygens as the *local environ-*

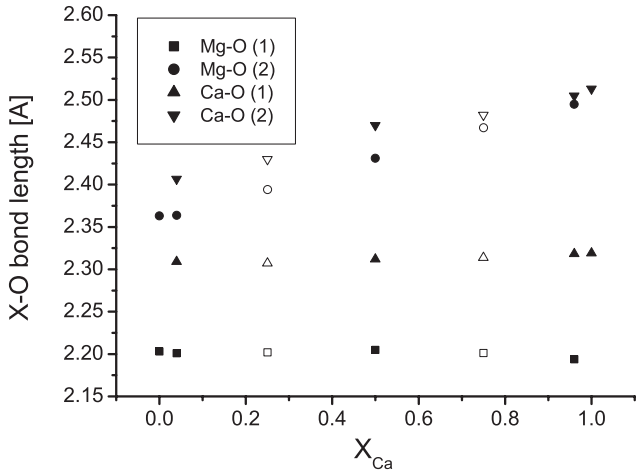

FIG. 5. Variation of the *X*-O (*X*=Mg, Ca) bond lengths with the mole fraction of grossular in the solid solution. Hollow points indicate the values where only two configurations have been used to generate the average distances. The filled points use either 13 configurations (for the $Gr_{50}Py_{50}$) or use the only unique configuration studied.

TABLE IV. Selected mean interatomic distances (Å) in the SiO_4 tetrahedra separating Ca-Mg, Ca-Ca, and Mg-Mg third-NN combinations in the 13 configurations studied for the 50:50 composition of the pyrope-grossular solid solution. The distances listed, *A–D*, are labeled in Fig. 3.

Third-NN	Ca	Mg
A (O-O)	2.523	2.482
B (*X*-O)	2.325	2.187
C (Si-O)	1.622	1.624
D (Si-*X*)	2.973	2.848
Third-NN	Ca	Ca
A (O-O)	2.545	2.545
B (*X*-O)	2.305	2.309
C (Si-O)	1.619	1.618
D (Si-*X*)	2.923	2.925
Third-NN	Mg	Mg
A (O-O)	2.468	2.472
B (*X*-O)	2.209	2.219
C (Si-O)	1.629	1.628
D (Si-*X*)	2.896	2.902

ment, we conclude that this is essentially independent of the bulk composition of the solid solution. EXAFS analysis at the Ca *K* edge has suggested that the lengths of the Ca-O1 and Ca-O2 bonds converge with each other and the Mg-O2 bond length below ≈0.5 grossular mole fraction.[9] The picture that emerges from our first-principles calculations is rather different. We see a linear rather than non-linear variation in the *X*-O2 bond lengths, with no marked change at any particular composition. Due to the decrease of the Mg-O2 separation with increasing Mg content, the Mg-O2 and Ca-O1 bond lengths do get closer as the magnesium mole fraction rises, but at the 50:50 composition there is still an appreciable difference (≈0.1 Å). A difference of 0.05 Å persists *even in the dilute limit* (Mg:Ca 96:4). The Ca-O2 and Mg-O2 bond lengths are much more similar than Ca-O1 and Mg-O1 at all solid solution compositions, differing typically by a few hundredths of an angstrom, but nevertheless Ca-O2 remains slightly larger even in the dilute limit (Mg:Ca 4:96). Our results show that the *X*-O1 bond length is independent of the bulk composition of the garnet solid solution and we see no signs of convergence of the bond lengths of either Ca-O1 or Ca-O2 with the Mg-O2 bond length.

Close inspection of the same interatomic distances and angles associated with the SiO_4 tetrahedra recorded earlier for the end members reveals subtle changes. Recalling that each SiO_4 tetrahedron separates two third-NNs, we have averaged these separately for particular third-NN combinations (Ca-Mg, Ca-Ca and Mg-Mg) in the 13 configurations studied for the 50:50 pyrope-grossular composition. Values of distances *A–D* are listed in Table IV. Corresponding angles θ, ϕ, and φ (again as defined for the end members in Fig. 4) are given in Table V.

TABLE V. Selected average O-Si-O bond angles (degrees) in the SiO_4 tetrahedra separating Ca-Mg, Ca-Ca and Mg-Mg third-NN combinations in the 13 configurations studied for the 50:50 composition of the pyrope-grossular solid solution. The particular angles are defined in Fig. 4.

Third-NN interaction	Mg-Mg	Ca-Mg	Ca-Ca
θ	98.56	102.10	103.61
ϕ	98.84	99.78	103.74
φ	115.11	113.89	112.45
Mean deviation from 109.47° (see text)	7.35	5.79	3.92

We consider first structural changes associated with cations with identical third-NNs since this is the cation arrangement also present in the end members. These are represented schematically in Fig. 6. For Mg-Mg third-NNs [Fig. 6(a)], the Si-Mg separation is ≈1.4% larger in the 50:50 mixture than in pyrope, consistent with an increase in the mean lat-

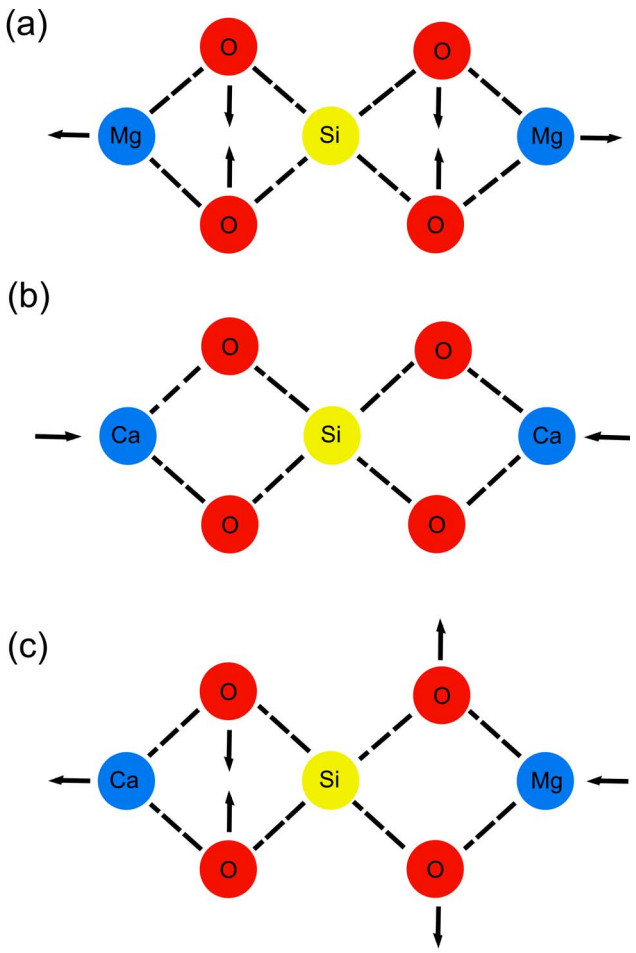

FIG. 6. (Color online) Changes in the structure of the solid solution relative to the respective end members associated with different third-NN interactions for (a) Mg-Mg third-NNs and (b) Ca-Ca third-NNs. (c) Changes in the structure associated with the Ca-Mg third-NN combination relative to those of the Ca-Ca and Mg-Mg third-NN combinations in the solid solution.

tice parameter a of 1.8%. Accompanying this overall increase in volume is an elongation of the chains made up of the dodecahedra and the SiO_4 tetrahedra. Thus the O-O separation is ≈0.4% smaller in the mixture, the Mg-O1 bond ≈0.5% longer. The O-Si-O bond angles θ and $\phi \approx 1.5°$ smaller and the mean deviation from the regular tetrahedral angle ≈1° larger. Thus, overall, the distortions of the SiO_4 tetrahedra associated with Mg-Mg third-NNs increase in the solid solution relative to those in pyrope itself.

The local structural environment associated with Ca-Ca third-NNs in the 50:50 solid solution is quite different [Fig. 6(b)]. The Ca-O1 bonds in the mixture are ≈0.5% shorter than in grossular but the O-O separation does not change. The O-Si-O bond angles θ and ϕ are now ≈1° closer to 109.47° and the mean deviation from the tetrahedral angle ≈0.5° smaller than in grossular. The chains made up of the dodecahedra and tetrahedra are not as elongated as in grossular due to the reduction in the cell size and overall the SiO_4 tetrahedra are less distorted.

When the third-NNs are different in the solid solution, the distortions are not just a combination of those on one side of Fig. 6(a) and the other of Fig. 6(b). Figure 6(c) shows the changes, this time not relative to the relevant end member, but to the Ca-Ca and Mg-Mg third-NN combinations in the solid solution [Fig. 6(a) and Fig. 6(b) respectively]. The Mg-O bonds are stiffer and require more energy to stretch than the Ca-O bonds, thus the Ca-O bonds now expand to accommodate the smaller Mg-O bonds. The Mg-O bonds are ≈1.2% smaller than in a solid solution Mg-Mg third-NN unit, while the Ca-O bonds are ≈0.8% longer than the Ca-O bonds in a Ca-Ca third-NN unit. The associated O-O separation is ≈0.5% larger for a Mg with a Ca third-NN than for a Mg with a Mg third-NN. Conversely, this O-O distance is ≈0.8% smaller for a Ca with a Mg third-NN than for a Ca with a Ca third-NN. The mean deviation of the O-Si-O bond angle from 109.47° is now 1.5° smaller for the tetrahedra between Ca-Mg third-NNs than for the tetrahedra between Mg-Mg third-NNs. The Ca side of the unit is more distorted than when the third-NN is Ca and this allows the Mg side of the unit to remain less distorted than in a Mg-Mg third-NN combination. The size of the distortion of the framework with each third-NN arrangement can be summarized by the mean modulus of the deviation of the O-Si-O bond angles from the perfect tetrahedral angle, as given in the final row of Table V. Overall, the SiO_4 tetrahedra are least distorted when both adjacent cations are Ca and are most distorted when both are Mg.

These results for the variations in the O-O separation, the X-O bond length and the O-Si-O bond angles are consistent with the often used qualitative argument that the smaller Mg cation is "too small" for the dodecahedral site.[25] Given the opportunity in the Ca-Mg third-NN arrangement, the Mg-O bonds contract relative to those in the Mg-Mg third-NN combination *and also relative to pyrope itself* at the expense of an increase in the Ca-O bond length and distortions in the O-Si-O bond angles. The Mg cations introduce strain into the structure as the framework distorts to accommodate them. We turn to consider the energetic consequences of this in the next section.

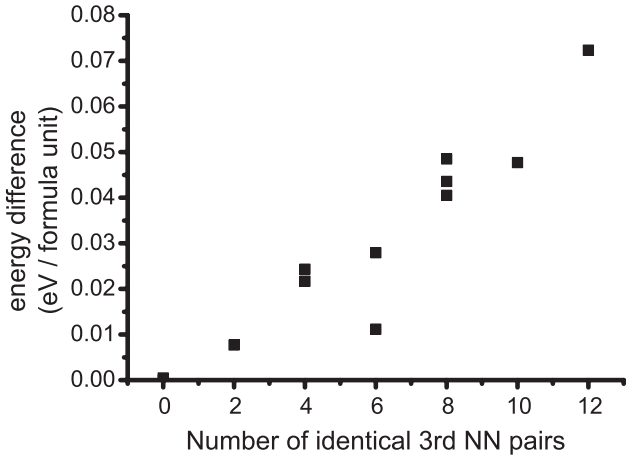

FIG. 7. The energy difference between each configuration and the lowest energy configuration vs the number of identical third-NN cations in the configuration. The lowest energy configuration is that with no identical third-NNs.

C. Solid solution: Energetics

The optimized energies of the 13 50:50 configurations are plotted versus the number of identical third-NNs (i.e., Ca-Ca and Mg-Mg) present in each configuration in Fig. 7. In agreement with other studies,[4,7,10] and as we anticipated above, in general, the more Mg-Mg and Ca-Ca third-NNs present in a particular configuration, the greater the energy of that configuration. The lowest energy configuration has no identical third-NN cations. The energy differences between the highest and lowest energy configurations are ≈0.08 eV per formula unit. The corresponding graph with energies for the same configurations obtained from classical simulations and the interatomic potentials used in our previous work[10] is very similar in form, but the energy differences are about three times those presented here. The relative magnitudes of the *ab initio* energies are more physically reasonable, suggesting that at ambient temperatures of 300 K only configurations with nearly all the cations arranged in Ca-Mg third-NN interactions are accessible. Complete randomization of the cations does not occur until temperatures in excess of 1000 K are reached. Bosenick *et al.*[12] have shown that the extent of local Ca-Mg ordering observed experimentally is a function of garnet synthesis temperature.

Thirteen configurations is usually too small a number to obtain accurate thermodynamic properties of mixing. Nevertheless, if we carry out a thermodynamic average over the *ab initio* energies of these configurations, as described in Refs. 28 and 29, we obtain a value of ≈6 kJ mol^{-1} for the enthalpy of mixing for the 50:50 composition at 1500 K. This is at least consistent with the admittedly widely scattered available experimental data[30] which suggests a value of ≈8 kJ mol^{-1}.

We can use the energies of these 13 different configurations to estimate the mean energy associated with the equilibrium shown in Eq. (1), in which a Ca-Ca third-NN unit and a Mg-Mg third-NN unit are replaced by two Ca-Mg third-NN combinations,

$$\frac{1}{2}\mathrm{Ca}-\mathrm{Ca}+\frac{1}{2}\mathrm{Mg}-\mathrm{Mg}\leftrightarrow 2\,\mathrm{Ca}-\mathrm{Mg}. \qquad (1)$$

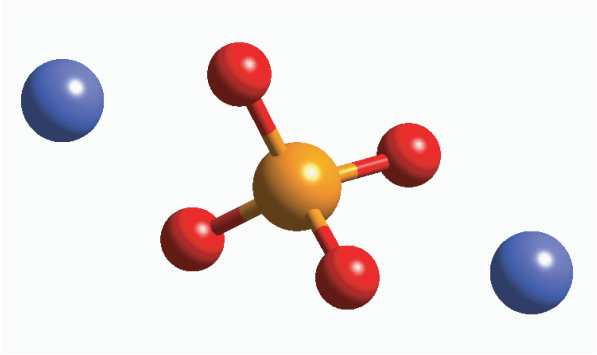

FIG. 8. (Color online) Structure of the cluster used for the HF and B3LYP calculations.

Using the energies of all the configurations, we obtain a small negative value of −0.44 eV for the energy change associated with reaction (1).

Since this calculation neglects any effects of changing nearest neighbors other than the third, we have also performed several single point *ab initio* molecular calculations on isolated A_2SiO_4 clusters. These clusters were constructed from the SiO_4 tetrahedra and adjoining cations from the thirteen optimized garnet configurations to make three different clusters (Mg_2SiO_4, $MgCaSiO_4$, Ca_2SiO_4) to represent the different third-NN arrangements (taken from the configurations with all the cations arranged with identical third-NNs or those without any identical third-NNs). Figure 8 shows the form of the clusters used. We have chosen not to relax the geometry of the cluster, since the relaxation of the isolated cluster could be quite different from that in the periodic system, but in each case used that obtained from the full structural optimizations and the earlier periodic *ab initio* calculations. Cluster calculations were carried out using both Hartree-Fock (HF) theory and at the Becke 3-Parameter (Exchange), Lee, Yang and Parr (correlation; density functional theory) (B3LYP) level of theory[31–34] using the JAGUAR program[35] and the LACVP basis set.[36] We use the resulting energies (given in Table VI) to determine the energy of Eq. (1) for the clusters. The calculated ΔU for this reaction is negative, in line with the periodic results: −0.231 eV (HF) and −0.218 eV (B3LYP).

Our analysis of the local geometry of the third-NN interaction shows that the largest distortion of the SiO_4 tetrahedra occurs when both third-NN are Mg and the smallest distortion occurs when both are Ca. The only difference between the 13 50:50 pyrope-grossular configurations studied is the location of the Ca and Mg cations. There are a total of 12 third-NN interactions in each configuration. For each Ca-Ca third-NN pair present, there must be a Mg-Mg third-NN pair to maintain the cation ratio of 1:1. Similarly, at any composition, the creation of an extra Ca-Ca third-NN interaction from a Ca-Mg pair necessarily involves also the formation of an Mg-Mg third-NN interaction. Thus the presence of the lower strain Ca-Ca third-NN necessarily results in the presence of the higher strain Mg-Mg third-NN so a system with the greatest number of "favorable" Ca-Ca interactions also possesses the greatest number of "unfavorable" Mg-Mg interactions. The negative value for the energy change associated with Eq. (1) shows that energetically the distortion introduced by two Ca-Mg third-NNs is less than that for the combination of a Mg-Mg third-NN and a Ca-Ca third-NN. The preferential ordering seen in the pyrope-grossular garnets thus effectively results from the avoidance of small Mg cations together as third-NN pairs.

TABLE VI. Energies of the molecular X_2SiO_4 (X=Mg, Ca) clusters studied calculated with both B3LYP and HF methods.

Third-NN pair	B3LYP (eV)	HF (eV)
Mg-Mg	−26933.32	−26851.05
Ca-Mg	−22488.74	−22410.82
Ca-Ca	−18043.72	−17970.12

It has been previously proposed by Bosenick *et al.*[7] and ourselves[37] that third-NNs comprising one large and one small cation (e.g., Ca-Mg), were energetically favored since identical third-NN units comprising Ca-Ca or Mg-Mg compressed or stretched the SiO_4 tetrahedra respectively. Our results here show this description needs modification. We have demonstrated that the Ca-Ca third-NN produces the least strain within the garnet lattice as measured by the distortion of the SiO_4 tetrahedra. A useful qualitative picture is that while the Mg can be regarded as "too small" for the dodecahedral site, the Ca is not "too large." The third-NN Ca-Mg cation ordering arises principally from avoiding only Mg-Mg third-NNs.

D. Cation incorporation

The third-NN cation arrangement has dramatic consequences for incorporation of foreign cations (trace elements) in the solid solution.[10,38,39] Substitution patterns in ionic solids generally obey Goldschmidt's rules[40] which state that the two main principles governing substitution are size (ionic radius) mismatch and charge difference between substituent and host. The greater the similarity between the cations, the more readily does substitution take place. We have previously carried out classical simulations[10,38,39] of the energetics of Eq. (2),

$$JO + Ca_{1.5}Mg_{1.5}Al_2Si_3O_{12} \leftrightarrow JCa_{0.5}Mg_{1.5}Al_2Si_3O_{12} + CaO \quad (2)$$

where J is a divalent cation, i.e., of the solution energies of binary oxides of divalent cations in the 50:50 garnet solid solution. These have established that small cations (e.g., Mg and Ni) substitute for a Ca rather than the similarly sized Mg when both third-NNs are also Ca. Conversely, larger cations (e.g., Ca, Sr, and Ba) substitute for Mg rather than Ca when both the third-NNs are Mg. The identity of the third-NN thus dictates the nature of substitution, dominating over the usual factors which lead to Goldschmidt's rules. Overall, these substitution patterns demonstrate an apparent unfavorable interaction when the third-NN cations in the garnet solid solution are identical or similar in size.

Our first-principles results suggest a modified interpretation for the *anti*-Goldschmidt behavior for the substitution of

large cations into the garnet solid solution.[10,38,39] A key factor is removal or avoidance of higher strain Mg-Mg third-NN interactions. A large cation such as Ba will remove a Mg-Mg third-NN pair, creating a Mg-Ba third-NN combination which overall causes a smaller distortion of the garnet framework. High strain third-NN combinations are also avoided when small cations are introduced. Consider also the incorporation of Ni, which is similar in size to Mg. Ni substitutes preferentially for Ca in a Ca-Ca third-NN pair rather than for Ca in a Ca-Mg third-NN pair as the latter involves the formation of the unfavorable Ni-Mg combination.[41]

IV. CONCLUSIONS

The *ab initio* calculations reported in this work have highlighted the crucial importance of the *local* environment of individual cations on the structure and energetics of the garnet solid solution. The results support those observed previously[7,10] from classical calculations that the energy of a particular configuration is closely related to the arrangement of the third-NN cations, even though these are separated by as much as ≈6 Å. By performing a detailed structural analysis of particular optimized solid solution configurations we offer an explanation for this trend. The SiO_4 tetrahedra between a cation and its third-NN are distorted and this distortion increases as the size of the cation or its third-NN decreases. The third-NN ordering favored in the Ca:Mg solid solution results from the avoidance of Mg-Mg third-NN interactions. We have also discussed the consequences for incorporation of foreign ions into the solid solution.

The smaller size of the Mg ion relative to that of Ca is the principal factor in causing distortion in the garnet framework. The same type of framework distortions might be expected in other garnets (e.g., the Fe^{2+} and Mn^{2+} end members almandine and spessartine) but of different magnitude. When the size differences between the cations are smaller, the difference between the various third-NN interactions will decrease, and *X*-cation ordering less extensive.

We have also investigated in detail the effect of solid solution composition on the *X*-cation local environment in the Ca:Mg solid solution. Our calculations indicate that the lengths of the shorter cation-O1 bonds are largely independent of the composition of the solid solution. The length of the longer cation-O2 bond varies almost linearly with composition, increasing with increasing grossular content. Due to the decrease of the Mg-O2 separation with increasing Mg content, the Mg-O2 and Ca-O1 bond lengths get closer together as the magnesium mole fraction rises but at the 50:50 composition an appreciable difference (≈0.1 Å) remains, and a difference of 0.05 Å persists even close to the dilute limit. This is in disagreement with the conclusions of Quartieri *et al.*[8] and Oberti *et al.*[9] who have interpreted their experimental EXAFS spectra in terms of a non-linear change in the Ca-O bond lengths with composition, resulting in the convergence of the Ca-O1 and Ca-O2 bond lengths with the Mg-O2 bond for mole fractions <0.5 grossular. Further experiments, or further analysis of existing data, would clearly be very worthwhile here.

ACKNOWLEDGMENTS

C.L.F. acknowledges support from EPSRC. Computational facilities for this work were made available by a number of EPSRC and HEFCE JREI grants to N.L.A. We would also like to thank Greg Ashby and Leonie Das for their contributions.

[1] A. M. Hofmeister and A. Chopelas, Am. Mineral. **76**, 880 (1991).
[2] A. Bosenick and C. A. Geiger, J. Geophys. Res., [Solid Earth] **102**, 22649 (1997).
[3] C. A. Geiger, in *Solid Solutions in Silicate and Oxide Systems*, edited by C. A. Geiger, EMU Notes in Mineralogy, Vol. 3 (Eötvös University Press, Budapest, 2001), chap. 4, pp. 71–100.
[4] M. H. F. Sluiter, V. Vinograd, and Y. Kawazoe, Phys. Rev. B **70**, 184120 (2004).
[5] G. V. Gibbs and J. V. Smith, Am. Mineral. **50**, 2023 (1965).
[6] L. Ungaretti, M. Leona, M. Merli, and R. Oberti, Eur. J. Mineral. **7**, 1299 (1995). This paper discusses in detail changes observed experimentally in the shape of the SiO_4 tetrahedra as a function of the nature of the cations at the *X*, *Y*, and *Z* sites.
[7] A. Bosenick, M. T. Dove, and C. A. Geiger, Phys. Chem. Miner. **27**, 398 (2000).
[8] S. Quartieri, M. C. Dalconi, F. Boscherini, R. Oberti, and F. D'Acapito, Phys. Chem. Miner. **31**, 162 (2004).
[9] R. Oberti, S. Quartieri, M. C. Dalconi, F. Boscherini, G. Iezzi, and M. Boiocchi, Chem. Geol. **225**, 347 (2006).
[10] W. van Westrenen, N. L. Allan, J. D. Blundy, M. Yu. Lavrentiev, B. R. Lucas, and J. A. Purton, Phys. Chem. Miner. **30**, 217 (2003).
[11] A. Bosenick, C. A. Geiger, T. Schaller, and A. Sebald, Am. Mineral. **80**, 691 (1995).
[12] A. Bosenick, C. A. Geiger, and B. L. Phillips, Am. Mineral. **84**, 1422 (1999).
[13] V. L. Vinograd, M. H. F. Sluiter, B. Winkler, A. Putnis, U. Hålenius, J. D. Gale, and U. Becker, Miner. Mag. **68**, 101 (2004).
[14] A. Beltrán, J. Andrés, J. G. Igualada, and J. Carda, J. Phys. Chem. **99**, 6493 (1995).
[15] Ph. D. D'Arco, F. F. Fava, R. Dovesi, and V. R. Saunders, J. Phys.: Condens. Matter **8**, 8815 (1996).
[16] R. H. Nobes, E. V. Akhmatskaya, V. Milman, B. Winkler, and C. J. Pickard, Comput. Mater. Sci. **17**, 141 (2000).
[17] V. Milam, E. V. Akhmatskaya, R. H. Nobes, B. Winkler, C. J. Pickard, and J. A. White, Acta Crystallogr., Sect. B: Struct. Sci. **57**, 163 (2001).
[18] Unfortunately Ref. 7 gives no details of the electronic structure calculations so no detailed comparisons with this work are possible. It is worth pointing out that these calculations were only used to obtain relative atomic interaction constants as listed in Table 6 of Ref. 7, but in this table the number and separations of all the nearest neighbors after the fifth are different from our own study of the garnet cell.
[19] M. C. Payne, M. P. Teter, D. C. Allan, T. A. Arias, and J. D. Joannopoulos, CASTEP 4.2, academic version, licensed under the

UKCP-MSI Agreement, 1999; Rev. Mod. Phys. **64**, 1045 (1992).
[20] J. P. Perdew and Y. Wang, Phys. Rev. B **45**, 13244 (1992).
[21] D. Vanderbilt, Phys. Rev. B **41**, R7892 (1990).
[22] H. J. Monkhorst and J. D. Pack, Phys. Rev. B **13**, 5188 (1976).
[23] L. Zhang, H. Ahsbahs, and A. Kutoglu, Phys. Chem. Miner. **25**, 301 (1998).
[24] J. Ganguly, W. Cheng, H., and St. C. O'Neill, Am. Mineral. **78**, 583 (1993).
[25] The "excess entropy" relates to measurements indicating that the heat capacity of pyrope exceeded that of grossular at low temperatures [E. F. Westrum, Jr., E. J. Essene, and D. Perkins, J. Chem. Thermodyn. **11**, 57 (1979)]. More recent experiments [A. M. Hofmeister and A. Chopelas, Am. Mineral. **76**, 880 (1991)] have not observed this.
[26] G. V. Gibbs and J. V. Smith, Am. Mineral. **50**, 2023 (1965).
[27] C. L. Freeman, Ph.D. thesis, University of Bristol, 2005.
[28] N. L. Allan, G. D. Barrera, R. M. Fracchia, M. Yu. Lavrentiev, M. B. Taylor, I. T. Todorov, and J. A. Purton, Phys. Rev. B **63**, 094203 (2001).
[29] I. T. Todorov, N. L. Allan, M. Yu. Lavrentiev, C. L. Freeman, C. E. Mohn, and J. A. Purton, J. Phys.: Condens. Matter **16**, S2751 (2004).
[30] R. C. Newton, T. V. Charlu, and O. L. Kleppa, Geochim. Cosmochim. Acta **41**, 369 (1977).
[31] A. D. Becke, J. Chem. Phys. **98**, 5648 (1993).
[32] C. Lee, W. Yang, and R. G. Parr, Phys. Rev. B **37**, 785 (1988).
[33] S. H. Vosko, L. Wilk, and M. Nusair, Can. J. Phys. **58**, 1200 (1980).
[34] P. J. Stephens, F. J. Devlin, and C. F. Chabalowski, J. Phys. Chem. **98**, 11623 (1994).
[35] JAGUAR 5.5, Schrödinger Inc., Portland, Oregon, 1991–2003.
[36] P. J. Hay and W. R. Wadt, J. Chem. Phys. **82**, 299 (1985).
[37] N. L. Allan, Z. Du. M. Yu. Lavrentiev, J. D. Blundy, J. A. Purton, and W. van Westrenen, Phys. Earth Planet. Inter. **130**, 93 (2003).
[38] W. van Westrenen, N. L. Allan, J. D. Blundy, M. Yu. Lavrentiev, B. R. Lucas, and J. A. Purton, Chem. Commun. (Cambridge) **2003**,786.
[39] C. L. Freeman, M. Yu. Lavrentiev, N. L. Allan, J. A. Purton, and W. van Westrenen, J. Mol. Struct.: THEOCHEM **727**, 199 (2005).
[40] V. M. Goldschmidt, J. Chem. Soc. **140**, 655 (1937).
[41] Why does Ni not substitute for Mg? Strain is not involved here. Substitution for Mg in an Mg-Mg or a Ca-Mg pair does not take place primarily since an Mg-O bond is substantially stronger than a Ca-O bond. Since the coordination of any cation is ≈ 8 (i.e., $4\times O1+4\times O1$) in the garnet and only 6 in the binary oxide, to a first approximation each cation forms two more bonds in the former than in the latter. There is thus an extra energy penalty associated with substitution by Ni at a Mg site.